

Neutrino signal of electron-capture supernovae from core collapse to cooling

L. Hüdepohl,¹ B. Müller,¹ H.-T. Janka,¹ A. Marek,¹ and G. G. Raffelt²

¹Max-Planck-Institut für Astrophysik, Karl-Schwarzschild-Str. 1, D-85748 Garching, Germany

²Max-Planck-Institut für Physik, Werner-Heisenberg-Institut, Föhringer Ring 6, D-80802 München, Germany

(Dated: October 22, 2018)

An $8.8 M_{\odot}$ electron-capture supernova was simulated in spherical symmetry consistently from collapse through explosion to essentially complete deleptonization of the forming neutron star. The evolution time (~ 9 s) is short because high-density effects suppress our neutrino opacities. After a short phase of accretion-enhanced luminosities (~ 200 ms), luminosity equipartition among all species becomes almost perfect and the spectra of $\bar{\nu}_e$ and $\bar{\nu}_{\mu,\tau}$ very similar, ruling out the neutrino-driven wind as r-process site. We also discuss consequences for neutrino flavor oscillations.

PACS numbers: 97.60.Bw, 95.85.Ry, 26.30.-k, 97.60.Jd

Introduction.—During the first seconds after collapse, a supernova (SN) core emits its binding energy, roughly 10% of its rest mass, in the form of neutrinos. In the delayed explosion paradigm, supported at least for some progenitor stars by recent simulations [1], neutrinos revive the stalled shock wave and by their energy deposition explode the star [2]. Later they drive a powerful wind and through β -processes determine its role as a possible site for r-process nucleosynthesis [3]. Inevitable deviations from spherical symmetry allow the neutrino flux to emit gravitational waves [4] and to impart a potentially large neutron-star recoil [5].

A sparse neutrino signal was observed from SN 1987A. Existing and foreseen large detectors [6] will operate for decades, suggesting the next galactic SN will provide a high-statistics signal and allow for a direct glance of its inner workings. The cosmic diffuse neutrino background from all past SNe (DSNB) is almost certainly detectable if gadolinium loading of Super-Kamiokande succeeds [7] or by future large scintillator detectors [8], pushing the frontiers of neutrino astronomy to cosmic distances.

The fluxes and spectra differ for the species ν_e , $\bar{\nu}_e$ and ν_x (representing any of $\nu_{\mu,\tau}$ or $\bar{\nu}_{\mu,\tau}$). Flavor oscillations swap $\nu_e \leftrightarrow \nu_x$ and $\bar{\nu}_e \leftrightarrow \bar{\nu}_x$ in part or completely, a process strongly affected by collective effects and Mikheev-Smirnov-Wolfenstein resonances [9]. What is seen in the neutrino-driven wind or by a detector thus depends not only on what is emitted, but also on the matter profile and neutrino mixing parameters.

Quantitative studies in these areas are impeded by large uncertainties of the expected fluxes and spectra. This problem partly derives from uncertainties of the explosion mechanism itself and input physics such as the nuclear equation of state (EoS). Significant variations are expected in dependence of the progenitor mass, and sometimes rotation and magnetic fields may come into play. However, even without such complications, the range of predictions is large for the post-explosion cooling phase when by far most of the neutrino loss happens.

The pioneering work of the Livermore group combined relativistic hydrodynamics with multi-group three-flavor

neutrino diffusion in spherical symmetry (1D), simulating the entire evolution self-consistently [10]. The spectra were hard over a period of at least 10 s with increasing hierarchy $\langle \epsilon_{\nu_x} \rangle > \langle \epsilon_{\bar{\nu}_e} \rangle > \langle \epsilon_{\nu_e} \rangle$. These models, however, included significant numerical approximations and omitted neutrino reactions that were later recognized to be important [11]. A crucial ingredient to enhance the early neutrino fluxes was a neutron-finger mixing instability, which today is disfavored [12].

Relativistic calculations of proto neutron star (PNS) cooling with a flux-limited equilibrium [13, 14] or multi-group diffusion treatment [15] found monotonically decreasing neutrino energies after no more than a short ($\lesssim 100$ ms) period of increase. Pons et al. [16] studied PNS cooling for different EoS and masses, using flux-limited equilibrium transport with diffusion coefficients adapted to the underlying EoS. They always found spectral hardening over 2–5 s before turning over to cooling.

New opportunities to study the neutrino signal consistently from collapse to late-time cooling arise from the class of “electron-capture SNe” (ECSNe) or “O-Ne-Mg core SNe.” These low-mass ($8\text{--}10 M_{\odot}$) stars collapse because of rapid electron capture on Ne and Mg and could represent up to 30% of all SNe [17]. They are the only cases where 1D simulations obtain neutrino-powered explosions [18] and 2D yields only minor dynamical and energetic modifications [19]. It has become possible to carry hydrodynamic simulations with modern neutrino Boltzmann solvers in 1D all the way to PNS cooling.

Very recently, the Basel group has circulated first results of the PNS evolution [20] for a representative $8.8 M_{\odot}$ progenitor [21] using Shen et al.’s EoS [22], which is relatively stiff and yields cold NS radii around 15 km.

Here we present our own long-term simulations of the same progenitor and the same EoS, facilitating a direct comparison (results with different EoS will be reported elsewhere). We will show that improved neutrino interaction rates lead to significant differences.

Numerical method.—Our simulations were performed with the PROMETHEUS/VERTEX code. It couples an explicit third-order Riemann-solver-based Newtonian hy-

drodynamics code with an implicit multi-flavor, multi-energy-group two-moment closure scheme for neutrino transport. The variable Eddington-factor closure is obtained from a model Boltzmann equation [23]. We account for general relativistic (GR) corrections with an effective gravitational potential (case A of Ref. [24]) and the transport includes GR redshift and time dilation. Tests showed good overall agreement until several 100 ms after core bounce [24, 25] with fully relativistic simulations of the Basel group’s AGILE-BOLTZTRAN code. A more recent comparison with a GR program [26] that combines the CoCoNUT hydro solver [27] with the VERTEX neutrino transport, reveals almost perfect agreement except for a few quantities with deviations of at most 7–10% until several seconds. The total neutrino loss of the PNS agrees with the relativistic binding energy of the NS to roughly 1%, defining the accuracy of global energy and lepton-number conservation in our simulations.

Our primary case (Model Sf) includes the full set of neutrino reactions described in Appendix A of Ref. [28] with the original sources. In particular, we account for nucleon recoils and thermal motions, nucleon-nucleon (NN) correlations, weak magnetism, a reduced effective nucleon mass and quenching of the axial-vector coupling at high densities, NN bremsstrahlung, $\nu\nu$ scattering, and $\nu_e\bar{\nu}_e \rightarrow \nu_{\mu,\tau}\bar{\nu}_{\mu,\tau}$. In addition, we include electron capture and inelastic neutrino scattering on nuclei [29].

To compare with previous simulations and the Basel work [20] we also consider in Model Sr a reduced set of opacities, omitting pure neutrino interactions and all mentioned improvements of the neutrino-nucleon interactions relative to the treatment of [30].

Long-term simulations.—In Fig. 1 we show the evolution of the ν_e , $\bar{\nu}_e$ and ν_x luminosities and of the average energies, defined as the ratio of energy to number fluxes. The dynamical evolution, development of the explosion, and shock propagation were previously described [18, 19]. The characteristic phases of neutrino emission are clearly visible: (i) Luminosity rise during collapse. (ii) Shock breakout burst. (iii) Accretion phase, ending already at ~ 0.2 s post bounce when neutrino heating reverses the infall. (iv) Kelvin-Helmholtz cooling of the hot PNS with a duration of 10 s or more, accompanied by mass outflow in the neutrino-driven wind.

The PNS evolves in the familiar way [13, 16] through deleptonization and energy loss. It contracts, initially heating up by compression and down-scattering of energetic ν_e produced in captures of highly degenerate electrons. With progressing neutronization the PNS cools, approaching a state of β -equilibrium with vanishing ν_e chemical potential μ_{ν_e} and minimal electron content.

In Model Sf, deleptonization and cooling take ~ 10 s until ν transparency is approached. For $t > 8.9$ s we find $T \lesssim 6$ MeV and $\mu_{\nu_e} \sim 0$ throughout, and $\dot{N}_L \ll 10^{53} \text{ s}^{-1}$. The final baryon mass is $M_b = 1.366 M_\odot$ with radius ~ 15 km. Neutrinos have carried away lepton number

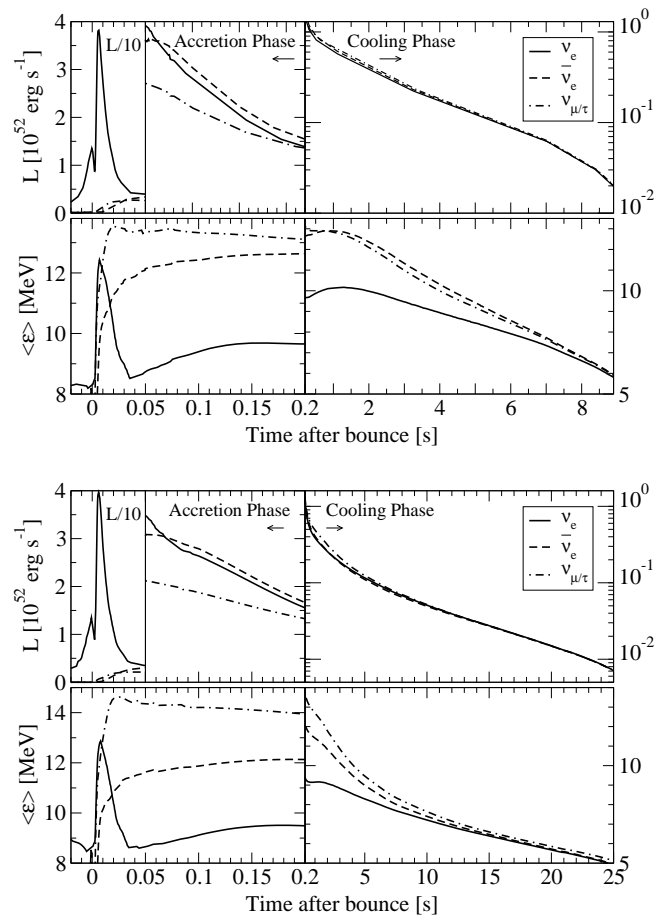


FIG. 1: Neutrino luminosities and mean energies observed at infinity. *Top*: Full set of neutrino opacities (Model Sf). *Bottom*: Reduced set (Model Sr).

of 6.57×10^{56} and energy $E_\nu = 1.66 \times 10^{53}$ erg, so the gravitational mass is $M = M_b - E_\nu/c^2 = 1.273 M_\odot$. The evolution is faster than in previous works [16] or in Model Sr because the high-density ν opacities are suppressed, where NN correlations [31] probably dominate. In Model Sr, deleptonization continues at 25 s on the low level of $\dot{N}_L \lesssim 10^{53} \text{ s}^{-1}$, $T_{\text{center}} \sim 11.5$ MeV, and only 97% of the gravitational binding energy have been lost.

Differences are also conspicuous in the luminosities. Until 5.5 s they are higher (up to 60% at $t \sim 2$ s) in Model Sf, whereas afterwards they drop much faster compared to Model Sr. On the other hand, for $t \gtrsim 0.2$ s, after the end of accretion, the luminosities in both models become independent of flavor within 10% or better. The total radiated E_ν shows nearly equipartition: 20% are carried away by ν_e , 16% by $\bar{\nu}_e$, and $4 \times 16\%$ by ν_x .

Spectra.—The mean neutrino energies evolve very differently in the two cases. While they increase over 1–1.5 s for ν_e and $\bar{\nu}_e$ in Model Sf, they increase only until ~ 0.2 s in Model Sr. The opacities are lower and thus the neutrino spheres at higher T , so Model Sf has larger $\langle \epsilon_{\nu_e} \rangle$ and $\langle \epsilon_{\bar{\nu}_e} \rangle$ for several seconds before dropping below Model Sr

due to the faster overall evolution.

The canonical spectral hierarchy $\langle \epsilon_{\nu_x} \rangle > \langle \epsilon_{\bar{\nu}_e} \rangle > \langle \epsilon_{\nu_e} \rangle$ persists in Model Sr during the cooling phase, while in Model Sf we find $\langle \epsilon_{\nu_x} \rangle \approx \langle \epsilon_{\bar{\nu}_e} \rangle > \langle \epsilon_{\nu_e} \rangle$. The close similarity and actually slight cross over of $\langle \epsilon_{\nu_x} \rangle$ and $\langle \epsilon_{\bar{\nu}_e} \rangle$ is caused by ν energy transfer in $\nu N \rightarrow N\nu$. As recognized previously [11], this in particular suppresses the high-energy tail of the ν_x spectrum (spectral pinching) and reduces $\langle \epsilon_{\nu_x} \rangle$ because the ν_x energy sphere is at higher density and surrounded by a thick scattering layer.

A quasi-thermal spectrum can be characterized by its lowest energy moments $\bar{\epsilon} \equiv \langle \epsilon_{\nu} \rangle$ and $\langle \epsilon_{\nu}^2 \rangle$. Simple analytic fits use a nominal Fermi-Dirac (FD) distribution with temperature T and degeneracy parameter η [32] or a modified power law $f_{\alpha}(\epsilon) = (\epsilon/\bar{\epsilon})^{\alpha} e^{-(\alpha+1)\epsilon/\bar{\epsilon}}$ [11]. The spectrum is “pinched” (narrower than a thermal FD) if $p = a^{-1} \langle \epsilon_{\nu}^2 \rangle / \langle \epsilon_{\nu} \rangle^2 = a^{-1} (2 + \alpha) / (1 + \alpha) < 1$ where $a \approx 1.3029$. So it is pinched for $p < 1$, $\eta > 0$ and $\alpha \gtrsim 2.3$ and anti-pinched otherwise. A Maxwell-Boltzmann (MB) spectrum has $\alpha = 2$, $\eta = -\infty$ and $p \approx 1.0234$.

In Model Sf the ν_e spectrum is always pinched, while $\bar{\nu}_e$ and ν_x are mildly anti-pinched ($-1 < \eta < 0$) for $3 \text{ s} \lesssim t \lesssim 7 \text{ s}$ (Fig. 2). At the end of the simulation $\langle \epsilon \rangle$ becomes almost identical for all species. The same applies to the spectral shape, which approaches a thermal FD function ($\alpha \approx 2.5$, $p \approx 0.99$, $\eta \approx 0.6$).

The time-integrated spectra of the number fluxes have $\langle \epsilon_{\nu_e, \bar{\nu}_e, \nu_x} \rangle = 9.40, 11.44, \text{ and } 11.44 \text{ MeV}$. The spectrum is moderately pinched for ν_e ($p \approx 0.96$, $\alpha \approx 3.0$, $\eta \approx 1.7$), a nearly thermal FD for $\bar{\nu}_e$ ($p \approx 0.99$), and slightly anti-pinched for ν_x ($p \approx 1.017$, $\alpha \approx 2.1$, $\eta \approx -1.5$).

Effective radiating surface.—The neutrino luminosities L_{ν} and effective temperatures T_e can be used to estimate the NS circumferential radius R . (This does not apply to late-time volume emission and the early accretion-powered phase.) The Stefan-Boltzmann law is $L_{\nu} = 4\pi\phi\sigma_{\nu}T_e^4R_{\infty}^2$ in terms of quantities measured at infinity and $\sigma_{\nu} = 4.751 \times 10^{35} \text{ erg MeV}^{-4} \text{ cm}^{-2} \text{ s}^{-1}$ if T_e is measured in MeV. A MB spectrum is assumed ($T_e = \frac{1}{3} \langle \epsilon_{\nu} \rangle$) with isotropic emission at the radiating surface. All deviations from these assumptions are absorbed in a “grayness factor” ϕ .

We define R as the location where $\rho = 10^{11} \text{ g cm}^{-3}$. GR corrections imply that $R_{\infty} = R/\sqrt{1 - 2\beta}$ where $\beta = GM/(Rc^2)$ and M is the PNS gravitational mass. In Model Sf, R/R_{∞} drops from an initial value near 1 to 0.88 at 3 s, followed by a slow decline to 0.87 at 8 s. M is linked to the gravitational binding energy and thus to the total ν energy release by $E_{\nu} \approx 0.6\beta Mc^2(1 - 0.5\beta)^{-1}$ [33], reproduced very well in our simulations. We propose to use these relations with measured values of E_{ν} , $\langle \epsilon_{\bar{\nu}_e} \rangle$ and $L_{\bar{\nu}_e}$ during the cooling phase to determine M and R from the signal of a future galactic SN.

The grayness factors for Model Sf are shown in Fig. 2. Their time variation is considerable, but $\phi \approx 0.6$ is a good choice for $\bar{\nu}_e$ around the time (5–6 s) of the $\alpha(t)$

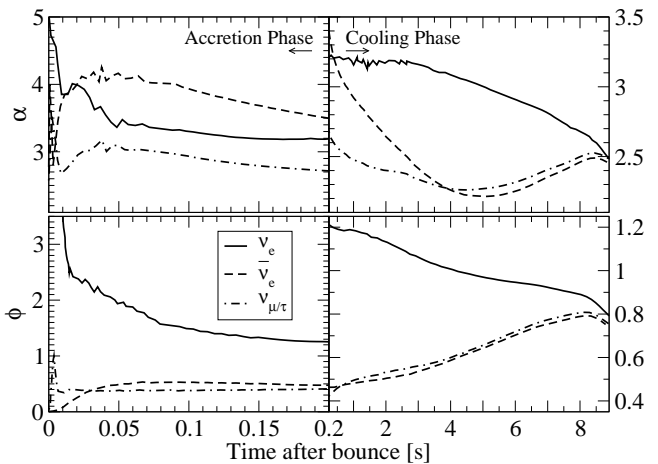


FIG. 2: Spectral fit parameter α and luminosity grayness factor ϕ for Model Sf.

minimum. This estimate applies for different EoS that we have tested. We also found that the evolutions of $\alpha(t)$ and $\phi(t)$ are not sensitive to the EoS.

Neutrino-driven wind.—Absorption of ν_e and $\bar{\nu}_e$ on nucleons determines the n/p ratio $Y_e^{-1} - 1$ in the neutrino-driven wind [3], where Y_e is the electron/baryon ratio. R-process nucleosynthesis conditions depend on n/p in addition to the entropy per baryon s , the expansion timescale τ_{exp} (between $T = 0.5 \text{ MeV}$ and $0.5/e \text{ MeV}$), and the mass-loss rate \dot{M} , which in turn depend on the neutrino energy deposition [3].

Since $\langle \epsilon_{\nu_e} \rangle$ and $\langle \epsilon_{\bar{\nu}_e} \rangle$ are very similar and because $\bar{\nu}_e$ absorptions are impeded by the n/p mass difference, one finds Y_e values significantly above 0.5 [20]. We confirm this result in our Model Sf (Fig. 3). The mean energies approach each other at late times, so Y_e grows monotonically and reaches ~ 0.63 after 9 s. Proton excess was suspected earlier [34] and in addition to insufficient entropies [35] disfavors r-processing even in the late wind. Flavor conversions of active neutrinos cannot change this

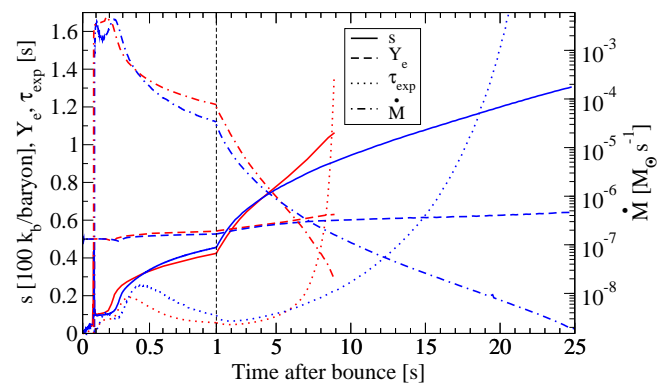


FIG. 3: Neutrino-driven wind properties (Model Sf: red, Model Sr: blue). τ_{exp} refers to the T -decline at 0.5 MeV. NOTE THE ERRATUM ON PAGE 5.

conclusion because $\langle \epsilon_{\bar{\nu}_e} \rangle \sim \langle \epsilon_{\bar{\nu}_x} \rangle$.

Conclusions.—Our simulations of an ECSN confirm that the difference between $\langle \epsilon_{\bar{\nu}_e} \rangle$ and $\langle \epsilon_{\nu_e} \rangle$ is too small for n-excess in the ν -driven wind, excluding ECSNe as r-process site [20]. When nucleon recoils are included (Model Sf), the mild hierarchy $\langle \epsilon_{\nu_x} \rangle > \langle \epsilon_{\bar{\nu}_e} \rangle > \langle \epsilon_{\nu_e} \rangle$ found in [20] and in our Model Sr changes to $\langle \epsilon_{\nu_x} \rangle \approx \langle \epsilon_{\bar{\nu}_e} \rangle > \langle \epsilon_{\nu_e} \rangle$. Thus flavor conversions in the $\bar{\nu}$ sector would hardly have any impact.

The PNS cooling time is significantly shortened by high-density nuclear effects in the neutrino opacities. A steep density but shallow T profile near the PNS surface causes ν_e , $\bar{\nu}_e$, and ν_x to be radiated from a thermal bath with similar neutrinospheric radii and temperatures. Luminosity equipartition among all species during the cooling phase is therefore almost perfect, compatible with [10] and [20] and despite different spectral hierarchies. Only during accretion-powered neutrino emission is $L_{\nu_e, \bar{\nu}_e}$ significantly larger than L_{ν_x} , and flavor oscillations would most easily show up in a high-statistics SN $\bar{\nu}_e$ signal during this phase. Differences between the ν_e and ν_x fluxes and spectra are pronounced in all phases. Therefore, a large ν_e detector would be especially useful [36].

The time-integrated $\langle \epsilon_{\bar{\nu}_e, \bar{\nu}_x} \rangle = 11.4$ MeV is relatively low. Results in [20] suggest that $\langle \epsilon_{\bar{\nu}_e, \bar{\nu}_x} \rangle = 11$ –12 MeV may be typical also for more massive progenitors and PNS. If so, the agreement with the SN1987A ν data would be much better than previously thought [37].

Our ECSN simulations with different softer and stiffer EoS (to be published elsewhere) yield similar results and corroborate our conclusions. The time-integrated $\langle \epsilon_{\bar{\nu}_e, \bar{\nu}_x} \rangle$ differs by no more than ~ 0.5 MeV.

Emission differences of ν_e and $\bar{\nu}_e$ and wind properties depend only modestly on the PNS mass up to nearly the black hole limit [3, 16, 35]. PNS winds with p-excess thus probably disfavor r-processing also in other SNe, as already seen for 10.8 and 18 M_\odot stars in [20]. Our simulations with PNS convection (to be reported elsewhere) also yield $Y_e > 0.5$, whereas $Y_e \lesssim 0.3$ is needed for a strong r-process with typical s and τ_{exp} values obtained in wind models [35, 38]. It remains to be explored if Y_e in common SNe can be sufficiently reduced by a new physical mechanism, perhaps involving rotation, magnetic fields or a modified composition (e.g. light clusters [39]).

We acknowledge partial support by DFG grants No. SFB/TR 7, SFB/TR 27, EXC 153 and computer time at the HLRS in Stuttgart and NIC in Jülich.

[1] H.-T. Janka *et al.*, Phys. Rept. **442**, 38 (2007).
 [2] H. A. Bethe and J. R. Wilson, Astrophys. J. **295**, 14 (1985).
 [3] Y.-Z. Qian and S. E. Woosley, Astrophys. J. **471**, 331 (1996).
 [4] R. Epstein, Astrophys. J. **223**, 1037 (1978).

[5] D. Lai, D. F. Chernoff and J. M. Cordes, Astrophys. J. **549**, 1111 (2001). G. M. Fuller *et al.*, Phys. Rev. D **68**, 103002 (2003).
 [6] K. Scholberg, Proc. Neutrino 2006, astro-ph/0701081.
 [7] H. Watanabe *et al.* [Super-Kamiokande Collaboration], Astropart. Phys. **31**, 320 (2009).
 [8] D. Autiero *et al.*, JCAP **0711**, 011 (2007).
 [9] A. Dighe, J. Phys. Conf. Ser. **136**, 022041 (2008).
 [10] T. Totani *et al.*, Astrophys. J. **496**, 216 (1998). H. E. Dalhed, J. R. Wilson and R. W. Mayle, Nucl. Phys. Proc. Suppl. **77**, 429 (1999).
 [11] M. T. Keil, G. G. Raffelt and H.-T. Janka, Astrophys. J. **590**, 971 (2003).
 [12] S. W. Bruenn and T. Dineva, Astrophys. J. **458**, L71 (1996).
 [13] A. Burrows and J. M. Lattimer, Astrophys. J. **307**, 178 (1986).
 [14] W. Keil and H.-T. Janka, Astron. Astrophys. **296**, 145 (1995).
 [15] H. Suzuki, Num. Astrophys. in Japan **2**, 267 (1991); in *Frontiers of Neutrino Astrophysics*, ed. by Y. Suzuki and K. Nakamura (Univ. Acad. Press, Tokyo, 1993), p. 219.
 [16] J. A. Pons *et al.*, Astrophys. J. **513**, 780 (1999).
 [17] S. Wanajo *et al.*, Astrophys. J. **695**, 208 (2009). A. J. T. Poelarends *et al.*, Astrophys. J. **675**, 614 (2008).
 [18] F. S. Kitaura, H.-T. Janka and W. Hillebrandt, Astron. Astrophys. **450**, 345 (2006).
 [19] H.-T. Janka *et al.*, Astron. Astrophys. **485**, 199 (2008).
 [20] T. Fischer *et al.*, arXiv:0908.1871.
 [21] K. Nomoto, Astrophys. J. **277**, 791 (1984); **322**, 206 (1987).
 [22] H. Shen *et al.*, Nucl. Phys. A **637**, 435 (1998).
 [23] M. Rampp and H.-T. Janka, Astron. Astrophys. **396**, 361 (2002).
 [24] A. Marek *et al.*, Astron. Astrophys. **445**, 273 (2006).
 [25] M. Liebendörfer *et al.*, Astrophys. J. **620**, 840 (2005).
 [26] B. Müller, H.-T. Janka, and H. Dimmelmeier, arXiv:1001.4841
 [27] H. Dimmelmeier, J. A. Font and E. Müller, Astron. Astrophys. **388**, 917 (2002).
 [28] R. Buras *et al.*, Astron. Astrophys. **447**, 1049 (2006).
 [29] K. Langanke *et al.*, Phys. Rev. Lett. **90**, 241102 (2003). K. Langanke *et al.*, Phys. Rev. Lett. **100**, 011101 (2008).
 [30] S. W. Bruenn, Astrophys. J. Suppl. **58**, 771 (1985).
 [31] S. Reddy, M. Prakash and J. M. Lattimer, Phys. Rev. D **58**, 013009 (1998). S. Reddy *et al.*, Phys. Rev. C **59**, 2888 (1999). A. Burrows and R. F. Sawyer, Phys. Rev. C **58**, 554 (1998); **59**, 510 (1999).
 [32] H.-T. Janka and W. Hillebrandt, Astron. Astrophys. **224**, 49 (1989).
 [33] J. M. Lattimer and M. Prakash, Astrophys. J. **550**, 426 (2001).
 [34] C. J. Horowitz and G. Li, Phys. Rev. Lett. **82**, 5198 (1999).
 [35] T. A. Thompson, A. Burrows and B. S. Meyer, Astrophys. J. **562**, 887 (2001).
 [36] C. Lunardini, B. Müller, and H.-T. Janka, Phys. Rev. D **78**, 023016 (2008).
 [37] B. Jegerlehner, F. Neubig and G. Raffelt, Phys. Rev. D **54**, 1194 (1996).
 [38] R. D. Hoffman, S. E. Woosley and Y.-Z. Qian, Astrophys. J. **482**, 951 (1997).
 [39] A. Arcones *et al.*, Phys. Rev. C **78**, 015806 (2008).

Erratum

In the original paper, a factor of 4π was incorrectly omitted in computing the mass-loss rates \dot{M} plotted in Fig. 3. The corrected version of Fig. 3 is given here. This correction does not affect the conclusions of the Letter. No reference was actually made to numerical values of \dot{M} in the text.

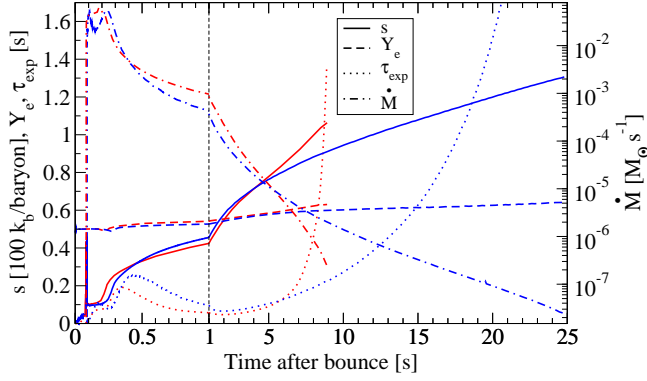


FIG. 3: Neutrino-driven wind properties (Model Sf: red, Model Sr: blue). τ_{exp} refers to the T -decline at 0.5 MeV.